GRATING MONOCHROMATOR FOR SOFT X-RAY SELF-SEEDING THE EUROPEAN XFEL

S. Serkez, V. Kocharyan and E. Saldin, DESY, Hamburg, Germany
G. Geloni, European XFEL GmbH, Hamburg, Germany

Abstract

Self-seeding implementation in the soft X-ray wavelength range involves gratings as dispersive elements. We study a very compact self-seeding scheme with a grating monochromator originally designed at SLAC, which can be straightforwardly installed in the SASE3 undulator beamline at the European XFEL. The design is based on a toroidal VLS grating at a fixed incidence angle, and without entrance slit. It covers the spectral range from 300 eV to 1000 eV. The performance was evaluated using wave optics method vs ray tracing methods. Wave optics analysis takes into account the actual beam wavefront of the radiation from the FEL source, third order aberrations, and errors from optical elements. We show that, without exit slit, the self-seeding scheme gives the same resolving power (about 7000) as with an exit slit. Wave optics is also naturally applicable to calculations of the scheme efficiency, which include the monochromator transmittance and the effect of the mismatching between seed beam and electron beam. Simulations show that the FEL power reaches 1 TW, with a spectral density about two orders of magnitude higher than that for the SASE pulse at saturation. A more detailed study and further references can be found in [1].

INTRODUCTION

Self-seeding is a promising approach to significantly narrow the SASE bandwidth and to produce nearly transform-limited pulses [2]-[11]. Considerable effort has been invested in theoretical investigation and $R\&D$ at the LCLS leading to the implementation of a hard X-ray self-seeding (HXRSS) setup that relies on a diamond monochromator in transmission geometry. Following the successful demonstration of the HXRSS setup at the LCLS [12], there is a need for an extension of the method in the soft X-ray range.

In general, a self-seeding setup consists of two undulators separated by a photon monochromator and an electron bypass, normally a four-dipole chicane. The two undulators are resonant at the same radiation wavelength. The SASE radiation generated by the first undulator passes through the narrow-band monochromator. A transform-limited pulse is created, which is used as a coherent seed in the second undulator. Chromatic dispersion effect in the bypass chicane smears out the microbunching in the electron bunch produced by the SASE lasing in the first undulator. The electrons and the monochromatized photon beam are recombined at the entrance of the second undulator, and radiation is amplified by the electron bunch until saturation is reached. The required seed power at the beginning of the second undulator must dominate over the shot noise power within the gain bandpass, which is order of a kW in the soft X-ray range.

For self-seeding in the soft x-ray range, proposed monochromators usually consists of a grating [2], [5]. Recently, a very compact soft x-ray self-seeding (SXRSS) scheme has appeared, based on grating monochromator [13]-[15]. The delay of the photons in the last SXRSS version [15] is about 0.7 ps only. The proposed monochromator is composed of only three mirrors and a toroidal VLS grating. The design adopts a constant, 1 degree incidence-angle mode of operation, in order to suppress the influence of movement of the source point in the first SASE undulator on the monochromator performance.

In this article we study the performance of the soft X-ray self-seeding scheme for the European XFEL upgrade. In order to preserve the performance of the baseline undulator, we fit the magnetic chicane within the space of a single 5 m undulator segment space at SASE3. In this way, the setup does not perturb the undulator focusing system. The magnetic chicane accomplishes three tasks by itself. It creates an offset for monochromator installation, it removes the electron microbunching produced in the upstream seed undulator, and it acts as an electron beam delay line for compensating the optical delay introduced by the monochromator. The monochromator design is compact enough to fit with this magnetic chicane design. The monochromator design adopted in this paper is an adaptation of the novel one by Y. Feng et al. [15], is based on toroidal VLS grating, and has many advantages. It consists of a few elements. In particular, it operates without entrance slit, and is, therefore, very compact. Moreover, it can be simplified further. Quite surprisingly, a monochromatic seed can be directly selected by the electron beam at the entrance of the second undulator. In other words, the electron beam plays, in this case, the role of an exit slit. By using a wave optics approach and FEL simulations we show that the monochromator design without exit slits works in a satisfactory way.

With the radiation beam monochromatized down to the Fourier transform limit, a variety of very different techniques leading to further improvement of the X-ray FEL performance become feasible. In particular, the most promising way to extract more FEL power than that at saturation is by tapering the magnetic field of the undulator [16]-[22]. A significant increase in power is achievable by starting the FEL process from a monochromatic seed rather than from shot noise [20]-[27]. In this paper we propose a study of the soft X-ray self-seeding scheme for the European XFEL, based on start-to-end simulations for an elec-

ISBN 978-3-95450-126-7

tron beam with 0.1 nC charge [28]. Simulations show that the FEL power of the transform-limited soft X-ray pulses may be increased up to 1 TW by properly tapering the baseline (SASE3) undulator. In particular, it is possible to create a source capable of delivering fully-coherent, 10 fs (FWHM) soft X-ray pulses with 10^{14} photons per pulse in the water window.

The availability of free undulator tunnels at the European XFEL facility offers a unique opportunity to build a beamline optimized for coherent diffraction imaging of complex molecules like proteins and other biologically interesting structures. Full exploitation of these techniques require 2 keV - 6 keV photon energy range and TW peak power pulses. However, higher photon energies are needed to reach anomalous edges of commonly used elements (such as Se) for anomalous experimental phasing. Potential users of the bio-imaging beamline also wish to investigate large biological structures in the soft X-ray photon energy range down to the water window. A conceptual design for the undulator system of such a bio-imaging beamline based on self-seeding schemes developed for the European XFEL was suggested in [29]-[30]. The bio-imaging beamline would be equipped with two different self-seeding setups, one providing monochromatization in the hard x-ray wavelength range, using diamond monochromators and one providing monochromatization in the soft x-ray range using a grating monochromator. In relation to this proposal, we note that the design for a soft x-ray self-seeding scheme discussed here can be implemented not only at the SASE3 beamline but, as discussed in [29]-[30], constitutes a suitable solution for the bio-imaging beamline in the soft x-ray range as well.

SELF-SEEDING SETUP DESCRIPTION

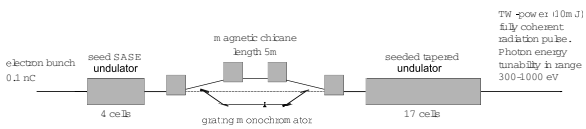

Figure 1: Design of the SASE3 undulator system for TW mode of operation in the soft X-ray range.

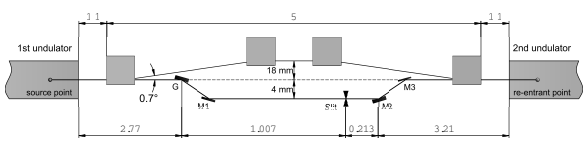

Figure 2: Layout of the SASE3 self-seeding system, to be located in the space freed after removing the undulator segment U5. The compact grating monochromator design relies on a scheme originally proposed at SLAC. G is a toroidal VLS grating. M1 is a rotating plane mirror, M2 is a tangential cylindrical mirror, M3 is a plane mirror used to steer the beam. The deflection of both electron and photon beams is in the horizontal direction.

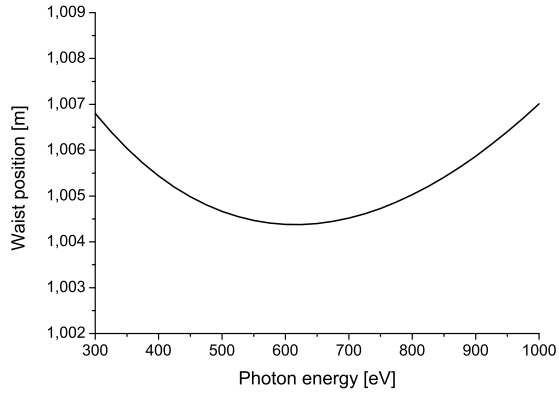

Figure 3: Focusing at the slit. Distance between waist, characterized by plane wavefront, and grating as a function of the photon energy.

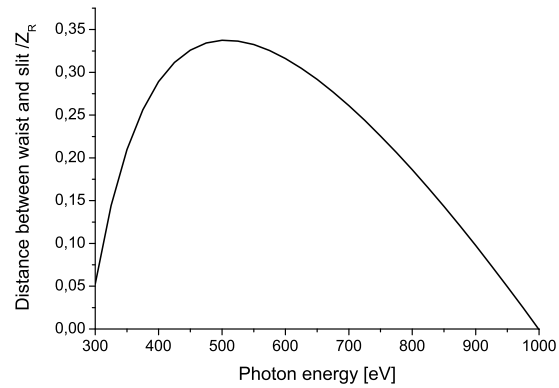

Figure 4: Focusing at the slit. Variation of the distance between waist and slit normalized on the Rayleigh range as a function of the photon energy.

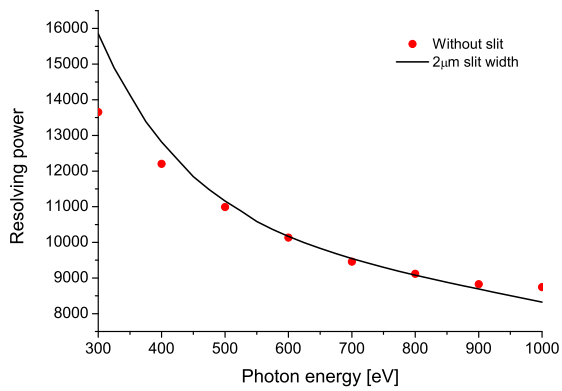

Figure 5: Resolving power as a function of the photon energy for a monochromator equipped with exit slit (bold curve) and without exit slit (circles). The calculation with exit slit is for a slit width of 2μm.

A design of the self-seeding setup based on the undulator system for the European XFEL baseline is sketched

ISBN 978-3-95450-126-7

Table 1: Parameters for the X-ray Optical Elements

Element	Parameter	Value at photon energy			Required precision	Unit
		300 eV	600 eV	1000 eV		
G	Line density (k)	1123			0.2%	l/mm
G	Linear coeff (n_1)	2.14			1%	l/mm^2
G	Quad coeff (n_2)	0.003			50%	l/mm^3
G	Groove profile	Blased 1.2°			-	-
G,M1	Roughness (rms)	-			2	nm
G	Tangential radius	160			1%	m
G	Sagittal radius	0.25			10%	m
G	Diffraction order	+1				-
G	Incident angle	1			-	deg
G	Exit angle	5.615	4.028	3.816	-	deg
	Source distance[1]	3160	3470	3870	-	mm
	Source size	30.3	27.7	24.2	-	μm
	Image distance[1]	1007	1004	1007	-	mm
	Image size	2.22	2.45	2.22	-	μm
M1	Location[1,2]	33.2	43.8	52.6	-	mm
M1	Incident angle	3.307	2.514	2.093	-	deg
S	Slit location[1]	1007			0.5	mm
S	Slit width	2			5%	μm
M2	Location[1]	1220			1	mm
M2	Incident angle	0.859			-	deg
M2	Tangential radius	27.3			1%	m
M3	Location[1]	1348.3			-	mm
M3	Incident angle	0.859			-	deg
	Optical delay	935	757	662	-	fs

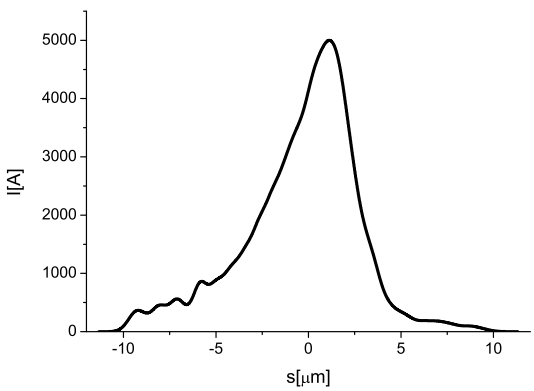

Figure 6: Current profile for a 100 pC electron bunch at the entrance of the first undulator.

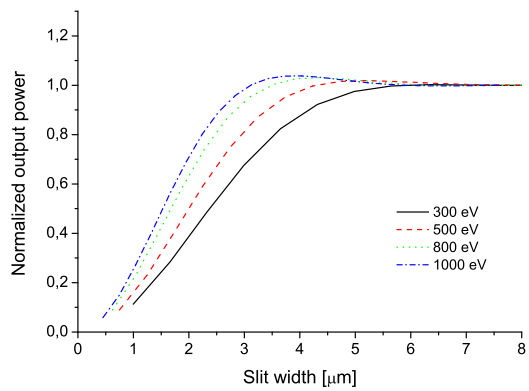

Figure 7: Results of seeding efficiency simulations, showing the normalized output power from the second FEL amplifier as a function of the exit slit width for different photon energies. The FEL amplifier operates in the linear regime. Results are obtained by wave optics and FEL simulations.

in Fig. 1. The method for generating highly monochromatic, high power soft x-ray pulses exploits a combination of a self-seeding scheme with grating monochromator with an undulator tapering technique. The self-seeding setup is composed by a compact grating monochromator originally proposed at SLAC [15], yielding about 0.7 ps optical delay, and a 5 m-long magnetic chicane.

[1]Distance to grating.
[2]Principal ray hit point.

Usually, a grating monochromator consists of an entrance slit, a grating, and an exit slit. The grating equation, which describes how the monochromator works, relies on the principle of interference applied to the light coming from the illuminated grooves. Such principle though, can

ISBN 978-3-95450-126-7

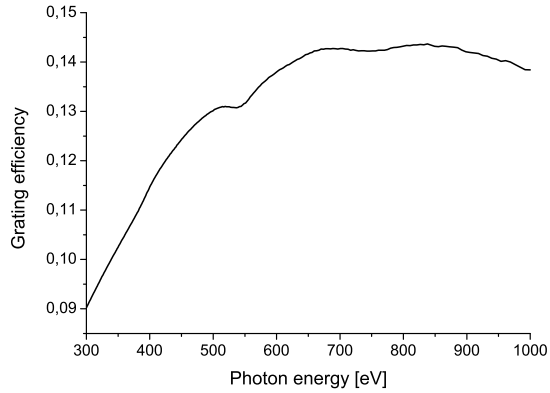

Figure 8: First order efficiency of the blazed groove profile. Here the groove density is 1100 lines/mm, Pt coating is assumed, at an incidence angle of 1°. The blaze angle is 1.2°; the anti-blaze angle is 90°.

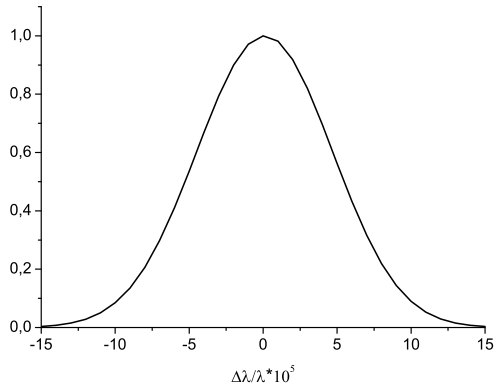

Figure 10: Line profile of the self-seeding monochromator without exit slit. The calculation is for a photon energy of 0.8 keV. The overall efficiency of the monochromator beamline is about 5%.

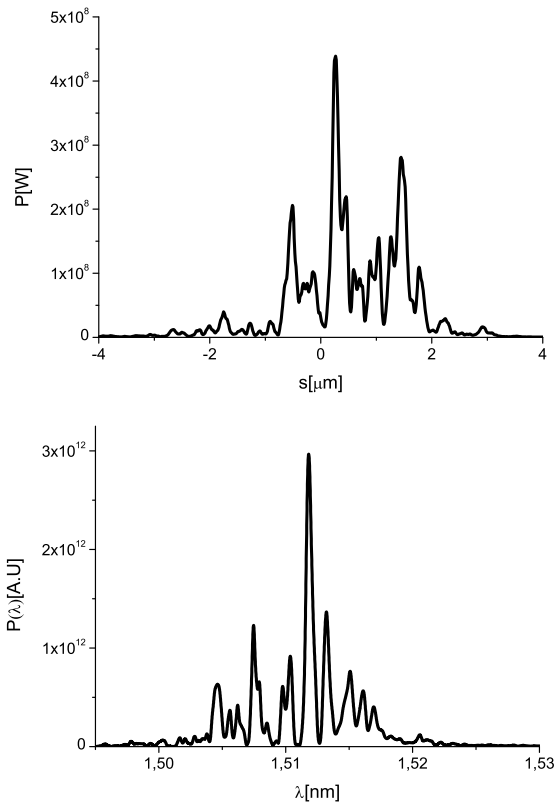

Figure 9: Power distribution and spectrum of the SASE soft x-ray radiation pulse at the exit of the first undulator.

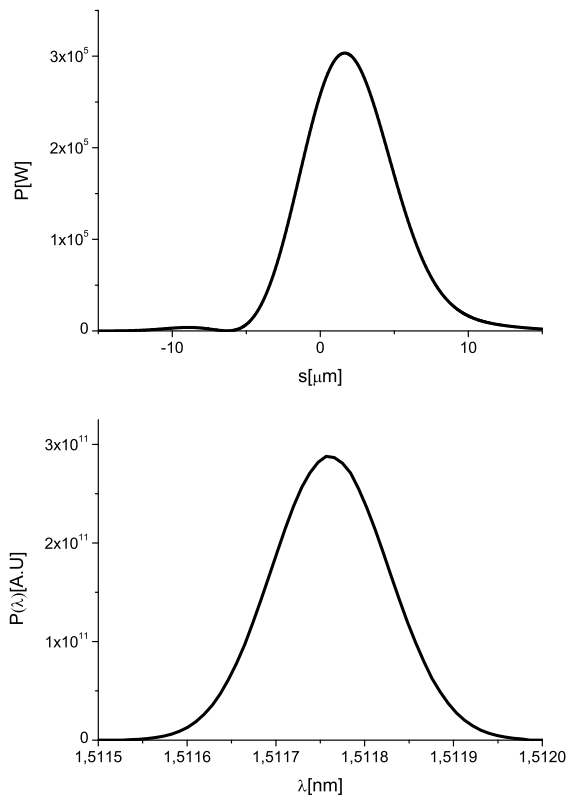

Figure 11: Power distribution and spectrum of the SASE soft x-ray radiation pulse after the monochromator. This pulse is used to seed the electron bunch at the entrance of the second undulator.

only be applied when phase and amplitude variations in the electromagnetic field are well-defined across the grating, that is when the field is perfectly transversely coherent. The purpose of the entrance slit is to supply a transversely coherent radiation spot at the grating, in order to allow the monochromator to work with an incoherent source and with a given resolution. However, an FEL source is highly transversely coherent and no entrance slit is required in this case [31, 32].

Figure 2 shows the optical configuration of the self-seeding monochromator. Table 1 summarizes the optical parameters of the setup. The design of the monochromator was optimized with respect to the resolving power and the seeding efficiency. The design energy range of the monochromator is in the 0.3 keV - 1 keV interval with a

ISBN 978-3-95450-126-7

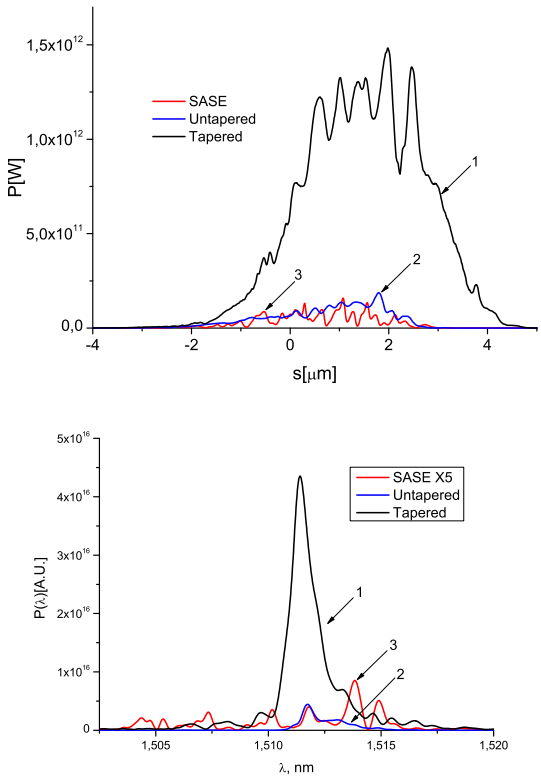

Figure 12: Power distribution and spectrum of the output soft x-ray radiation pulse. Curve 1 - seeded FEL output with tapering; curve 2 - seeded FEL output without tapering; curve 3 - SASE FEL output in saturation. Here $\lambda = 1.5$ nm, corresponding to 800 eV.

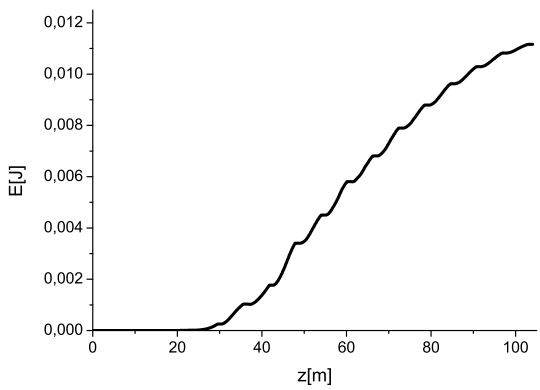

Figure 13: Energy of the seeded FEL pulse as a function of the distance inside the output undulator.

resolution of about 7000. It is only equipped with an exit slit. A toroidal grating with variable line spacing (VLS) is used for imaging the FEL source to the exit slit of the monochromator. The grating has a groove density of 1120 lines/mm. The first coefficient D_1 of the VLS grating is $D_1 = 2.1/\mathrm{mm}^2$. The grating will operate in fixed incident angle mode in the $+1$ order. The incident X-ray beam is imaged at the exit slit and re-imaged at the entrance of the seed undulator by a cylindrical mirror M2. In the sagittal plane, the source is imaged at the entrance of the seed undulator directly by the grating. The monochromator scanning is performed by rotating the post-grating plane mirror. The scanning results on a wavelength-dependent optical path. Therefore, a tunability of the path length in the magnetic chicane in the range of 0.05 mm is required to compensate for the change in the optical path.

The choice was made to use a toroidal VLS grating similar to the LCLS design [15]. As pointed out in that reference, the source point in the SASE undulator moves upstream with the photon energy. The proposed design has been chosen in order to minimize the variation of the image distance. The object distance was based on FEL simulations of the SASE3 undulator at the exit of the fourth segment U4, Fig. 1. The monochromator performance was calculated using wave optics. The exact location of the waist, characterized by a plane wavefront, Fig. 3 and Fig. 4, was found to vary with the energy around the slit within 2.7 mm, which is small compared to the Rayleigh range, Fig. 4. This defocusing effect was fully accounted for in the wave optics treatment, and the impact of this effect on the resolving power is negligible. The resolving power achievable with the exit slit is shown in Fig. 5. It approaches 8000, and is sufficient to produce temporally transform-limited seed pulses with FWHM duration between 25 fs and 50 fs over the designed photon energy range. This duration is sufficiently longer than the FWHM duration of the electron bunch, about 15 fs in standard mode of operation at 0.1 nC charge, Fig. 6. The resolving power depends on the size of the FEL source inside the SASE undulator, on the size of the exit slit (assumed fixed at 2μm) and on third order optical aberrations.

The operation of the self-seeding scheme involves simultaneous presence of monochromatized radiation and electron beam in the seed undulator. This suggests to consider a particularly interesting approach to solve the task of creating a monochromatized seed. In fact, the resolving power needed for seeding can be achieved without exit slit by combining the presence of radiation and electron beam in the seed undulator. The influence of the spatial dispersion in the image plane at the entrance of the seed undulator on the operation of the self-seeding setup without exit slit can be quantified by studying the input coupling factor between the seed beam and the ground mode of the FEL amplifier. A combination of wave optics and FEL simulations is the only method available for designing such self-seeding monochromator without exit slit. This design has the advantage of a much needed experimental simplicity,

ISBN 978-3-95450-126-7

and could deliver a resolving power as that with the exit slit. The comparison of resolving powers for these two designs is shown in Fig. 5. The size of the beam waist near the slit is about 2.2-2.4 μm. The operation without exit slit would give worse resolving power than the conventional mode of operation only when the slit size is smaller than 2 μm. Wave optics and FEL simulations are naturally applicable also for calculating suppression of the input coupling factor, due to the effect of a finite size of the exit slit. The effect of the slit on the seeding efficiency shown in Fig. 7. When the slit size is smaller than 2 μm, the effective seed power is reduced by as much as a factor $2-3$. We conclude that the mode of operation without exit slit is superior to the conventional mode of operation, and a finite slit size would only lead to a reduction of the monochromator performance.

The efficiency of the grating should be specified over the range of photon energies where the grating will be used. The efficiency was optimized by varying the groove shapes. Blazed grating was optimized by adjusting the blaze angle; sinusoidal grating by adjusting the groove depth, and rectangular grating by adjusting the groove depth, and assuming a duty cycle of 50%. The blazed profile is substantially superior to both sinusoidal and laminar alternatives. For the specified operating photon energy range, the optimal blaze angle is 1.2 degree, and the expected grating efficiency with platinum coating is shown in Fig. 8. This curve assumes a constant incident angle of 1 degree.

The electron beam chicane contains four identical dipole magnets, each of them 0.5 m-long. Given a magnetic field $B = 0.8T$ and an electron momentum $p = 10$GeV/c, this length corresponds to a dipole bending angle of 0.7 degrees. The choice of the strength of the magnetic chicane only depends on the delay that we want to introduce. In our case, as already mentioned, it amounts to 0.23 mm, or 0.7 ps. Parameters discussed above fit with a short, 5 m-long magnetic chicane to be installed in place of a single undulator module. Such chicane, albeit very compact, is however strong enough to create a sufficiently large transverse offset for the installation of the optical elements of the monochromator.

Despite the unprecedented increase in peak power of the X-ray pulses at SASE X-ray FELs some applications, including bio-imaging , require still higher photon flux [33]-[37]. The most promising way to extract more FEL power than that at saturation is by tapering the magnetic field of the undulator. Tapering consists in a slow reduction of the field strength of the undulator in order to preserve the resonance wavelength, while the kinetic energy of the electrons decreases due to FEL process. The undulator taper could be simply implemented at discrete steps from one undulator segment to the next. The magnetic field tapering is provided by changing the undulator gap. Here we study a scheme for generating TW-level soft X-ray pulses in a SASE3 tapered undulator, taking advantage of the highly monochromatic pulses generated with the self-seeding technique, which make the tapering very efficient. We optimized our setup based on start-to-end simulations for an electron beam with 100 pC charge. In this way, the output power of SASE3 could be increased from the baseline value of 100 GW to about a TW in the photon energy range between 0.3 keV and 1 keV.

Summing up, the overall self-seeding setup proposed here consists of three parts: a SASE undulator, a self-seeding grating monochromator and an output undulator in which the monochromtic seed signal is amplified up to the TW power level. Calculations show that in order not to spoil the electron beam quality and to simultaneously reach signal dominance over shot noise, the number of cells in the first (SASE) undulator should be equal to 4. The output undulator consists of two sections. The first section is composed by an uniform undulator, the second section by a tapered undulator. The transform-limited seed pulse is exponentially amplified passing through the first uniform part of the output undulator. This section is long enough, 6 cells, in order to reach saturation, which yields about 100 GW power. Finally, in the second part of the output undulator the monochromatic FEL output is enhanced up to the TW power level taking advantage of a 3.5% taper of the undulator magnetic field over the last 11 cells after saturation.

Simulations were performed with the help of the Genesis code [38] running on a cluster in the following way: first we calculated the 3D field distribution at the exit of the first undulator, and downloaded the field file. Subsequently, we performed a temporal Fourier transformation followed by filtering through the monochromator, by using the filter amplitude transfer function. The electron microbunching is washed out by presence of non-zero chicane momentum compaction factor R_{56}. Therefore, for the second undulator we used a beam file with no initial microbunching, and with an energy spread induced by the FEL amplification process in the first SASE undulator. The amplification process in the second undulator starts from the seed field-file. Shot noise initial conditions were included. The output power and spectrum after the first (SASE) undulator tuned at 1.5 nm is shown in Fig. 9. The instrumental function is shown in Fig. 10. The shape of this curve was found as a response of the input coupling factor on the offset of the seed monochromatic beam at the entrance of the seed undulator due to spatial dispersion. The absolute value of the transmittance accounts for the absorption of the monochromatic beam in the grating and in the three mirrors, for a total of 5%. The influence of the transverse mismatching of the seed beam at the entrance of the seed undulator is accounted for by an additional suppression of the input coupling factor. The resolution of the self-seeding monochromator is good enough, and the spectral width of the filter is a few times shorter than the coherent spectral interval (usually referred to as "spike") in the SASE spectrum. Therefore, the seed radiation pulse is temporally stretched in such way that the final shape only depends on the characteristics of the monochromator. The temporal shape and spectrum of the seed signal are shown in Fig. 11. The over-

ISBN 978-3-95450-126-7

all duration of the seed pulse is inversely proportional to the bandwidth of the monochromator transmittance spectrum. The particular temporal shape of the seed pulse simply follows from a Fourier transformation of the monochromator transfer function. The output FEL power and spectrum of the entire setup, that is after the second part of the output undulator is shown in Fig. 12. The evolution of the output energy in the photon pulse as a function of the distance inside the output undulator is reported in Fig. 13. The photon spectral density for a TW pulse is about two orders of magnitude higher than that for the SASE pulse at saturation (see Fig. 12). Given the fact that the TW-pulse FWHM-duration is about 10 fs, the relative bandwidth is 3 times wider than the transform-limited bandwidth. There is a relatively large energy chirp in the electron bunch due to wakefields effect. Nonlinear energy chirp in the electron bunch induces nonlinear phase chirp in the seed pulse during the amplification process in the output undulator. Our simulations automatically include this effect. This phase chirp increases the time-bandwidth product by broadening the seeded FEL spectrum.

CONCLUSIONS

In this article we present a technical study for a soft x-ray self-seeding setup at the European XFEL based on [15]. In particular we focus on design and performance of a very compact self-seeding grating monochromator, based on the LCLS design, which has been adapted to the needs of the European XFEL. Usually, soft X-ray monochromators operate with incoherent sources and their design is based on the use of ray-tracing codes. However, XFEL beams are almost completely transversely coherent, and in our case the optical system was studied using a wave optics method in combination with FEL simulations to evaluate the performance of the self-seeding scheme. Our wave optics analysis takes into account the actual FEL beam wavefront, third order aberrations and surface errors from each optical elements. Wave optics together with FEL simulations are naturally applicable to the study the influence of finite slit size on the seeding efficiency. Most results presented in [15] were obtained in the framework of a Gaussian beam model, in combination with ray-tracing for Gaussian ray distribution. This is a very fruitful approach, allowing one for studying many features of the self-seeding monochromator by means of relatively simple tools. Using our approach, we give a quantitative answer to the question of the accuracy of the Gaussian beam model. It is also important to quantitatively analyze the filtering process without exit slit. Wave optics in combination with FEL simulations is the only method available to this aim. We conclude that the mode of operation without slit is superior to the conventional mode of operation, and a finite slit size would only lead to a reduction of the monochromator performance. We therefore propose an optimized design based on a toroidal VLS grating and three mirrors, without exit slit. The monochromator covers the range between 300 eV and 1000 eV, with a resolution never falling below 7000, and introduces a photon delay of only 0.7 ps. This allows the entire self-seeding setup to be fit into a single 5 m-long undulator segment. The overall performance of the setup is studied with the help of FEL simulations, which show that, in combination with post-saturation tapering, the SASE3 baseline at the European XFEL could deliver TW-class, nearly Fourier-limited radiation pulses in the soft X-ray range. Although we explicitly studied the a soft x-ray self-seeding setup for the SASE3 undulator baseline at the European XFEL, the same setup can be used without modifications also for the dedicated bio-imaging beamline, a concept that was proposed in [29]-[30] as a possible future upgrade of the European XFEL. A more detailed study and further references can be found in [1].

ACKNOWLEDGEMENTS

We thank Daniele Cocco, Paul Emma, Yiping Feng, Jerome Hastings, Philip Heimann and Jacek Krzywinski for useful discussions. We are grateful to Massimo Altarelli, Reinhard Brinkmann, Henry Chapman, Janos Hajdu, Viktor Lamzin, Serguei Molodtsov and Edgar Weckert for their support and their interest during the compilation of this work.

REFERENCES

[1] DESY 13-040, "Grating monochromator for soft X-ray self-seeding the European XFEL", http://arxiv.org/abs/1303.1392, (2013)

[2] J. Feldhaus et al., Optics. Comm. 140, 341 (1997).

[3] E. Saldin, E. Schneidmiller, Yu. Shvyd'ko and M. Yurkov, NIM A 475 357 (2001).

[4] E. Saldin, E. Schneidmiller and M. Yurkov, NIM A 445 178 (2000).

[5] R. Treusch, W. Brefeld, J. Feldhaus and U Hahn, Ann. report 2001 "The seeding project for the FEL in TTF phase II" (2001).

[6] A. Marinelli et al., Comparison of HGHG and Self Seeded Scheme for the Production of Narrow Bandwidth FEL Radiation, Proceedings of FEL 2008, MOPPH009, Gyeongju (2008).

[7] G. Geloni, V. Kocharyan and E. Saldin, "Scheme for generation of highly monochromatic X-rays from a baseline XFEL undulator", DESY 10-033 (2010).

[8] Y. Ding, Z. Huang and R. Ruth, Phys.Rev.ST Accel.Beams, vol. 13, p. 060703 (2010).

[9] G. Geloni, V. Kocharyan and E. Saldin, "A simple method for controlling the line width of SASE X-ray FELs ", DESY 10-053 (2010).

[10] Geloni, G., Kocharyan, V., and Saldin, E., "Cost-effective way to enhance the capabilities of the LCLS baseline", DESY 10-133 (2010).

[11] Geloni, G., Kocharyan V., and Saldin, E., "A novel Self-seeding scheme for hard X-ray FELs", Journal of Modern Optics, vol. 58, issue 16, pp. 1391-1403, DOI:10.1080/09500340.2011.586473 (2011).

ISBN 978-3-95450-126-7

[12] J. Amann et al., Nature Photonics, DOI:10.1038/NPHOTON.2012.180 (2012).

[13] Y. Feng, J. Hastings, P. Heimann, M. Rowen, J. Krzywinski, and J. Wu, "X-ray Optics for soft X-ray self-seeding the LCLS-II", proceedings of 2010 FEL conference, Malmo, Sweden, (2010).

[14] Y. Feng, P. Heimann, J. Wu, J. Krzywinski, M. Rowen, and J. Hastings, "Compact Grating Monochromator Design for LCLS-I Soft X-ray Self-Seeding", https://slacportal.slac.stanford.edu/sites/lcls_public/lcls_ii/Lists/LCLS_II_Calendar/Physics_Meetings.aspx, May 2011 and https://sites.google.com/a/lbl.gov/realizing-the-potential-of-seeded-fels-in-the-soft-x-ray-regime-workshop/talks, October 2011

[15] Y. Feng et al., "System design for self-seeding the LCLS at soft X-ray energies", to appear in the Proceedings of the 24th International FEL Conference, Nara, Japan (2012).

[16] A. Lin and J.M. Dawson, Phys. Rev. Lett. 42 2172 (1986)

[17] P. Sprangle, C.M. Tang and W.M. Manheimer, Phys. Rev. Lett. 43 1932 (1979)

[18] N.M. Kroll, P. Morton and M.N. Rosenbluth, IEEE J. Quantum Electron., QE-17, 1436 (1981)

[19] T.J. Orzechovski et al., Phys. Rev. Lett. 57, 2172 (1986)

[20] W. Fawley et al., NIM A 483 (2002) p 537

[21] M. Cornacchia et al., J. Synchrotron rad. (2004) 11, 227-238

[22] X. Wang et al., PRL 103, 154801 (2009)

[23] G. Geloni, V. Kocharyan and E. Saldin, "Scheme for generation of fully coherent, TW power level hard x-ray pulses from baseline undulators at the European XFEL", DESY 10-108 (2010).

[24] Geloni, G., Kocharyan, V., and Saldin, E., "Production of transform-limited X-ray pulses through self-seeding at the European X-ray FEL", DESY 11-165 (2011).

[25] W.M. Fawley et al., Toward TW-level LCLS radiation pulses, TUOA4, to appear in the FEL 2011 Conference proceedings, Shanghai, China, 2011

[26] J. Wu et al., Simulation of the Hard X-ray Self-seeding FEL at LCLS, MOPB09, to appear in the FEL 2011 Conference proceedings, Shanghai, China, 2011

[27] Y. Jiao et al. Phys. Rev. ST Accel. Beams 15, 050704 (2012)

[28] I. Zagorodnov, "Beam Dynamics simulations for XFEL", http://www.dedy.de/sfel-beam/s2e (2011).

[29] G. Geloni, V. Kocharyan and E. Saldin, "Conceptual design of an undulator system for a dedicated bio-imaging beamline at the European X-ray FEL", DESY 12-082, http://arxiv.org/abs/1205.6345 (2012).

[30] G. Geloni, V. Kocharyan and E. Saldin, "Optimization of a dedicated bio-imaging beamline at the European X-ray FEL", DESY 12-159, http://arxiv.org/abs/1209.5972 (2012).

[31] C. Svetina, M. Zagrando, A. Bianco and D. Cocco, "A Fixed including angle monochromator for the 4th generation light source FERMI@ELETRA", Proc. of SPIE Vol. 7448, 74480.2009 (2009).

[32] M. Roper Nucl. Instruments and Methods in Physics Research A 635 580-587 (2011).

[33] J. Hajdu, Curr. Opin. Struct. Biol. 10, 569 (2000)

[34] R. Neutze et al., Nature 406, 752 (2000)

[35] K. J. Gaffney and H. N. Chapman, Science 316, 1444 (2007)

[36] M. M. Seibert et al., Nature 470 (7332) 78-81 (2011)

[37] S. Baradaran et al., LCLS-II New Instruments Workshops Report, SLAC-R-993 (2012), see Section 4.3.2. by H. Chapman et al., and Section 4.3.3. by F. R. N. C. Maia et al.

[38] S. Reiche et al., Nucl. Instr. and Meth. A 429, 243 (1999).

ISBN 978-3-95450-126-7